



Cite this: *Polym. Chem.*, 2023, **14**, 2054
2054

The effect of side chain spacer length on the thermoresponsive behaviour of poly(methylamide acrylate)s†

Alexander Rajakanthan, ^a Paul Wilson ^{*b} and Kristian Kempe ^{*a,c}

We report the synthesis of three methylamide acrylate monomers with varying spacer length between the polymerizable acrylate and pendant amide functionalities; methylamide ethyl acrylate (MAmEA), methylamide propyl acrylate (MAmPA) and methylamide butyl acrylate (MAmBA). Each monomer was subsequently polymerised *via* redox-initiated reversible addition-fragmentation chain transfer (RRAFT) to yield well-defined homopolymers with differing physicochemical properties. All homopolymers were found to be amorphous, and thermally degrade *via* a two-step decomposition process. Whilst P(MAmEA) and P(MAmPA) were found to be soluble in aqueous solution between 30–80 °C, P(MAmBA) showed a lower critical solution temperature (LCST) behaviour. Detailed aqueous solubility studies performed on P(MAmBA) revealed that the cloud point temperature (T_{cp}) could be tuned based on the degree of polymerisation (DP_n), concentration and nature of the aqueous media, highlighting its potential use as a water-soluble, thermoresponsive polymer in a range of applications.

Received 10th February 2023,
Accepted 29th March 2023
DOI: 10.1039/d3py00154g
rsc.li/polymers

Introduction

The development and discovery of novel water-soluble polymers is fundamental to the progression of a plethora of industries including pharmaceuticals, water treatment, cosmetics and agriculture.^{1–5} Water-soluble polymers can be classified into two categories based on their source; natural and synthetic. Whilst naturally sourced water-soluble polymers have been utilised for decades due to their high availability and biodegradation, recent advances in reversible deactivation radical polymerisation (RDRP) techniques have facilitated the synthesis of well-defined polymers with excellent control over their molecular weights and physicochemical properties,^{6–9} enabling the production of a wide range of functional, biocompatible, water-soluble polymers which have a range of applications.^{2,4} Furthermore, polymers which alter their physicochemical properties in response to changes in their local environment are especially significant. These materials are typically referred to as ‘smart’ polymers and previously synthesised examples have been responsive to numerous stimuli

such as temperature,^{10–12} pH^{13,14} and light.^{15,16} The most studied ‘smart’ polymers are temperature-responsive, typically referred to as thermoresponsive polymers. Thermoresponsive polymers are found to change their solubility in water at elevated or decreased temperatures due to conformational changes in the polymeric structure. The temperature at which conformational changes occur is referred to as the transition temperature. Thermoresponsive polymers thus display one of two transitions, or a combination of both: lower critical solution temperature (LCST) or upper critical solution temperature (UCST). Polymers displaying LCST behaviour are miscible in water and subsequently phase separate above the transition temperature.¹⁷ Conversely, polymers displaying UCST behaviour are insoluble in water and subsequently solubilise above the transition temperature.¹⁸ The most widely reported water-soluble polymer that exhibits an LCST behaviour is poly(*N*-isopropylacrylamide) (PNIPAm) owing to its rapid phase transition in water at 32 °C, which is significant for applications at physiological conditions.^{19,20} However, in this context, the significant hysteresis that occurs during PNIPAm’s phase transitions²¹ coupled with observed platelet adhesion²² and low blood compatibility²³ has resulted in the need for alternative biocompatible thermoresponsive polymers with LCST behaviour.

Well-studied alternatives include poly(ethylene glycol) (PEG),^{24,25} poly(*N*-vinyl-2-pyrrolidone) (PVP),^{26,27} and poly(2-oxazoline) (POx)²⁸ derivatives which all are non-ionic in nature and contain similar structural motifs. These polymer classes all possess hydrophilic functionalities in the polymer side

^aMonash Institute of Pharmaceutical Sciences, Monash University, 381 Royal Parade, Parkville, VIC 3052, Australia. E-mail: kristian.kempe@monash.edu

^bDepartment of Chemistry, University of Warwick, CV4 7AL, UK.
E-mail: p.wilson.1@warwick.ac.uk

^cDepartment of Material Science and Engineering, Monash University, Clayton, VIC 3800, Australia

† Electronic supplementary information (ESI) available. See DOI: <https://doi.org/10.1039/d3py00154g>

chain, which permit intramolecular and intermolecular hydrogen-bonding through, *e.g.* oxy-ether, amine, carbonyl and amide moieties. The magnitude of hydrogen-bonding afforded by these moieties will directly influence the temperature of the observed LCST.

An exciting new candidate is the recently resurrected polymer class of poly(amide acrylate)s (P(AmAs)), which contain secondary amide functionalities in their side chains. To date, the primary research focus into these materials has been the synthesis of electroactive polymers with self-healing properties.^{29–31} A very recent study on P(AmAs), which focused specifically on P(AmAs) that possess an ethyl spacer between the polyacrylate backbone and the amide functionality demonstrated their controlled (co)polymerisation *via* redox-initiated reversible addition fragmentation chain-transfer (RRAFT) polymerisation, which allowed to tailor their physicochemical properties.³² Importantly, it was shown that the type of alkyl amide functionality determines their water-solubility with poly(methylamide ethyl acrylate) (P(MAmEA)) being soluble over the measured temperature range, whilst poly(ethylamide ethyl acrylate) (P(EAmEA)), exhibited LCST behaviour. First cellular interaction studies of these polymers revealed their cytocompatibility and tuneable cellular association/uptake making them highly interesting candidates for future biomedical applications.

In the present study, we aimed to further explore this polymer class and investigate the effect of the spacer length between the polymer backbone and the amide functionality on the water-solubility of the resulting P(AmAs). To achieve high water-solubility the spacer length was varied from ethyl to butyl while the methylamide motif was selected for all systems. Homopolymers of two known monomers (MAmEA and MAmPA) were prepared in conjunction with that of a previously unreported monomer, methylamide butyl acrylate (MAmBA). All monomers were synthesised in high purity and subsequently polymerised *via* RRAFT polymerisation with high monomer conversion. All homopolymers exhibited high aqueous solubility at ambient conditions with varying temperature-responsivity at elevated temperatures. In contrast to P(MAmEA) and P(MAmPA), P(MAmBA) was found to show an LCST behaviour further highlighting the tuneability of this polymer class through simple alterations of the polymer structure.

Experimental

Materials

All chemicals were purchased from Sigma-Aldrich and used without further purification unless otherwise stated. Dialysis tubing (molecular weight cut-off, MWCO = 1 kDa) was purchased from Repligen. 2-((Butylthio)carbonothioyl)thio) propionic acid (BCTP) was purchased from Boron Molecular. Deuterated chloroform (CDCl_3) and deuterated water (D_2O) were purchased from Cambridge Isotope Labs. MAmEA, P(MAmEA) and MAmPA were synthesised according to literature.^{30,32}

Characterisation equipment

Nuclear magnetic resonance (NMR) spectroscopy of all samples were performed using a Bruker AVANCE III HD 400 MHz spectrometer at 25 °C running Bruker Topspin Software. Samples were prepared using CDCl_3 or D_2O . The spectra were processed *via* MestReNova software. Size exclusion chromatography (SEC) analysis of polymer solutions was performed using an Agilent 1260 Infinity II-MDS instrument equipped with differential refractive index (DRI), viscometry (VS), dual angle light scatter (LS) and multiple wavelength UV detectors. The system was equipped with 2× PLgel Mixed-D Columns (300 × 7.5 mm) and a PLgel 5 μm bead-size guard column. Dimethylformamide (DMF) with 5 mM NH_4BF_4 was used as the eluent where samples were run isocratically at 1 mL min^{-1} at 50 °C. Poly(methyl methacrylate) standards (PMMA; 0.55–955 kg mol⁻¹) were used for calibration. Analyte samples were filtered through 0.2 μm poly(tetrafluoroethylene) (PTFE) filters prior to injection. Experimental number average molecular weights ($M_{n,\text{SEC}}$) and dispersity (D_M) values of samples were determined on Agilent GPC/SEC software. Fourier transformed infrared spectroscopy (FT-IR) of all samples were performed using an Agilent Cary 630 FT-IR spectrometer with a diamond attenuated reflection cell. Thermogravimetric analysis (TGA) was carried out on a TA Instruments TGA with autosampler, under nitrogen flow (50 mL min^{-1}) at a heating rate of 10 °C min⁻¹. Samples were heated from 40 °C up to 1000 °C in 90 μL alumina pans. Differential scanning calorimetry (DSC) was carried out on a TA Instruments DSC with autosampler, under nitrogen flow (50 mL min^{-1}) at a heating rate of 10 °C min⁻¹. Samples were heated from -75 °C to 150 °C at a rate of 10 °C min⁻¹, cooling at 10 °C min⁻¹. Two cycles were performed using 40 μL aluminium pans and the second heating cycle of each sample was used to determine their glass-transition temperature (T_g). Turbidity measurements were performed using an Agilent Cary 60 UV-Vis spectrophotometer connected to a Quantum Northwest TC 1 temperature controller. All polymers were measured using the following conditions: wavelength, 600 nm; ramp, 1 °C min⁻¹; measurement wait time, 1 s; measurement interval, 0.1 °C. All cloud point temperatures (T_{cp}) recorded were determined on the 2nd heating cycle of each respective polymer solution. Water contact angle (CA) measurements were conducted at room temperature using a Krüss drop shape analysis system DSA100 equipped with a movable sample table and microliter syringe. Each polymeric film was produced by spin coating 500 μL of a polymer solution (10 mg ml⁻¹, MeOH) onto a clean glass slide for 5 min at 800 rpm using a Polos SPIN150i spin coater. Deionized water was used as the wetting liquid and the drop size was set to 3 μL . Polymeric films were placed onto the sample table and aligned within the field of view of the camera. The sample table was heated using a Krüss temperature control unit TC40 to either 25 °C or 75 °C. The microliter syringe was advanced until a droplet of 3 μL was formed at a rate of 3 $\mu\text{L s}^{-1}$ then subsequently suspended at the end of the syringe needle. The sample table was then elev-

ated, until the sample touched the bottom of the drop, causing it to detach from the end of the needle and form on the surface. The sample table was then moved back to the original position and an image immediately recorded. The baseline and contact angles were then computed from the image. This process was repeated five times for each sample and the reported values are the average taken from the repeat measurements.

Monomer synthesis

Synthesis of methylamide butyl acrylate, MAmBA

Acetic anhydride (6.30 g, 61.7 mmol, 1.1 eq.) was added dropwise to a suspension of aluminium oxide (\sim 5.0 g) and 4-amino-1-butanol (5.00 g, 56.1 mmol, 1.0 eq.) at 0 °C. The reaction mixture was stirred at room temperature for 10 min before removal of the aluminium oxide by filtration. After additional rinsing of the aluminium oxide with ethyl acetate, the organic phases were combined and the solvent was reduced *in vacuo* and dried over airflow yielding the product methylamide-1-butanol, MAmBOH, as a yellow oily liquid. Yield = 75%. 1 H NMR (400 MHz, CDCl_3): δ = 5.84 (H_f), 3.67 (H_g), 3.28 (H_d), 1.96 (H_a), 1.60 ($\text{H}_{e,f}$); 13 C NMR (400 MHz, CDCl_3): δ = 174.54 (C_b), 61.91 (C_g), 39.47 (C_d), 29.67 (C_e), 25.96 (C_f), 23.01 (C_a); FT-IR: cm^{-1} = 3290 (N–H), 1630 (NH–C=O). Acryloyl chloride (3.79 g, 41.9 mmol, 1.1 eq.) was then added dropwise to a solution of MAmBOH (5.0 g, 38.1 mmol, 1.0 eq.) and triethylamine (5.01 g, 49.6 mmol, 1.3 eq.) in anhydrous dichloromethane (50 mL) at 0 °C. The resulting mixture was allowed to come to room temperature, and stirring was continued for 16 h. Upon removal of the solvent, the crude was purified by flash column chromatograph (EtOAc/MeOH, gradient of 1–5% MeOH). The product MAmBA was obtained as a colourless liquid. Yield = 64%. 1 H NMR (400 MHz, CDCl_3): δ = 6.37 (H_g), 6.11 (H_g), 5.84 (H_g), 5.61 (H_c), 4.17 (H_e), 3.27 (H_d), 1.97 (H_a), 1.69 (H_h), 1.59 (H_i); 13 C NMR (400 MHz, CDCl_3): δ = 170.41 (C_b), 166.30 (C_f), 130.84 (C_g), 128.40 (C_g), 64.10 (C_e), 39.16 (C_d), 26.14 ($\text{C}_{h,i}$), 23.20 (C_a); FT-IR: cm^{-1} = 3300 (N–H), 1720 (O–C=O), 1650 (NH–C=O), 1180 (C–O), 810 (C=C).

Monomer self-association constant (K_a) studies

1 H NMR spectra of monomers were recorded at $[M] = 2.0 \text{ M}$, 1.0 M , 0.5 M , 0.2 M , 0.1 M , 0.05 M and 0.01 M . Samples were prepared *via* serial dilution of a 2.0 M stock solution of each monomer in dry CDCl_3 . A literature model was used to determine self-association constants (K_a) (eqn (S1)†).³³

Polymer synthesis

Synthesis of poly(methylamide acrylate) homopolymers by RRAFT

P(MAmBA)₉₉ was synthesised using the following method as a representative example:

MAmBA (300 mg, 1.62 mmol), BCTP (3.86 mg, 16.2 μmol) and AsAc (0.36 mg, 2.0 μmol) were added to a reaction vial equipped with a magnetic stirrer bar dissolved in deionized H_2O and 1,4-dioxane. The mixture was deoxygenated by bubbling with nitrogen for 15 min. In parallel, an aqueous stock solution of tBuOOH was deoxygenated. An aliquot of the latter (0.37 mg, 4.0 μmol) was added to the reaction vial *via* a nitrogen-purged syringe ($[M] : [CTA] : [t\text{BuOOH}] : [\text{AsAc}] = 100 : 1 : 0.25 : 0.125$). The resultant mixture was subsequently placed in a water bath at 25 °C for 24 h. 1 H NMR and SEC samples were taken to determine the conversion of the polymerisation and the molecular weight of the crude polymer, respectively. The resultant homopolymer was purified *via* dialysis (MWCO = 1 kDa) against Milli-Q water for two days. The purified product was isolated by lyophilisation as a white fluffy solid. Conversion: 99%. Yield = 70%. 1 H NMR (400 MHz, D_2O): δ = 4.13 (H_b), 3.22 (H_c), 2.33 (H_a), 2.00 (H_e), 1.69 (H_f), 1.59 (H_g); 13 C NMR (400 MHz, D_2O): δ = 176.34 (C_f), 173.28 (C_b), 65.07 (C_a), 38.88 (C_d), 25.57 (C_h), 25.22 (C_i), 21.94 (C_g); FT-IR: cm^{-1} = 3280 (N–H), 1730 (O–C=O), 1640 (NH–C=O), 1160 (C–O). Further synthetic detail related to Poly(methylamide acrylate) (P(MAmA)) homopolymers is provided in Table S1.†

Results and discussion

Monomer synthesis

Three methylamide acrylate monomers with varying spacer lengths between acrylate and amide functionalities were synthesised; MAmEA, MAmPA and MAmBA. MAmEA and MAmPA were synthesised according to literature and MAmBA was synthesised using an equivalent method.^{30,32} Each monomer was synthesised in a two-step procedure with the first step involving the amidation of a chosen alcohol amine using acetic anhydride (Fig. S1A†). 1 H NMR analysis of MAmBOH (Fig. S1B†) illustrated the introduced methyl protons (H_a) at 1.98 ppm whilst 13 C NMR analysis displayed the amide signals C_a and C_b at 23.01 ppm and 174.54 ppm respectively (Fig. S1C†). Furthermore, FT-IR analysis showed the appearance of amide N–H and C=O stretches at 3290 cm^{-1} and 1630 cm^{-1} respectively (Fig. S1D†). The second step involved the esterification of the terminal alcohol functionality with acryloyl chloride (Fig. 1A). Purification *via* flash column chromatography was optimized using an EtOAc/MeOH mobile phase to yield highly pure monomers. 1 H NMR analysis of MAmBA illustrated the introduced amide protons (H_c) at 5.61 ppm and vinyl protons (H_g) between 5.8–6.4 ppm (Fig. 1B). 13 C NMR analysis confirmed MAmBA synthesis *via* the introduced acrylate signals at 128.40 ppm (C_g), 130.84 ppm (C_g) and 166.30 ppm (C_f) (Fig. S2A†). Furthermore, the success of the reaction was confirmed *via* FT-IR spectroscopy (Fig. S2B†), which showed the appearance of ester C=O and C–O stretches at 1720 cm^{-1} and 1180 cm^{-1} respectively as well as a vinyl C=C stretch at 810 cm^{-1} .

Further 1 H NMR analysis of the secondary amide (R–NH–R') proton environment of each monomer (H_c) revealed a relation-

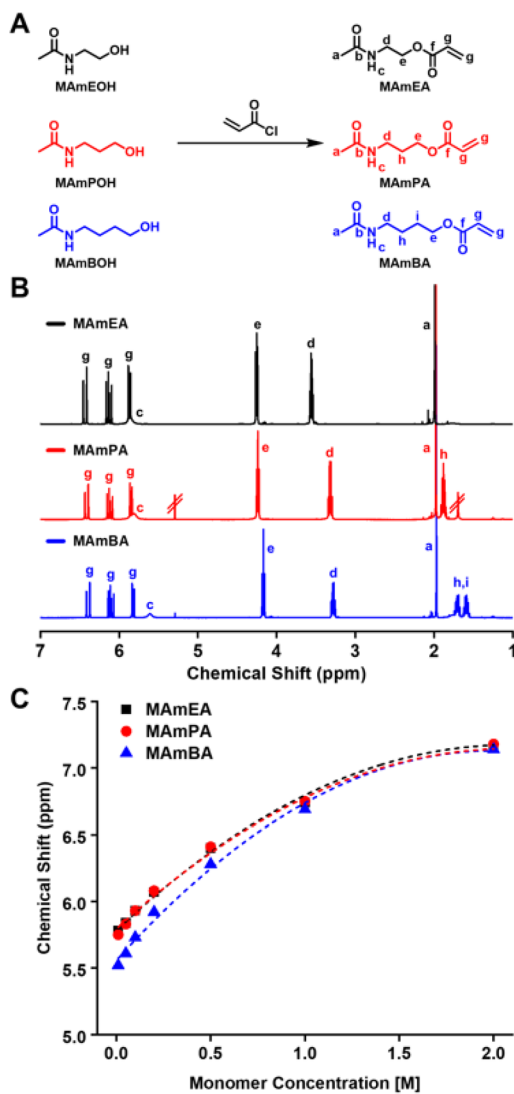


Fig. 1 (A) Synthesis pathway of monomers; (B) ¹H NMR spectra (400 MHz, CDCl₃) of MAmEA, MAmPA and MAmBA; (C) Concentration-dependent change in chemical shift of H_c of MAmEA ($K_a = 0.64 \text{ M}^{-1}$), MAmPA ($K_a = 0.52 \text{ M}^{-1}$) and MAmBA ($K_a = 0.38 \text{ M}^{-1}$) in CDCl₃. Dashed lines were added as visual aids.

ship between monomer concentration and its chemical shift value. This finding is consistent with previous literature on MAmPA, which reported that this phenomenon is due to intermolecular hydrogen-bonding interactions.³⁰ In dry organic solvents such as CDCl₃, increasing monomer concentration can induce dimerization. Consequently, in ¹H NMR spectroscopy, H_c will be observed at a higher chemical shift value if hydrogen-bonding between dimers is present. Conversely, H_c will be observed at a lower chemical shift value if the magnitude of hydrogen-bonding is decreased. The chemical shifts determined for MAmBA were consistently lower than for MAmEA and MAmPA at any given concentration (Fig. 1C, Fig. S3–5†). Thus, this indicates weaker intermolecular hydrogen-bonding in methylamide acrylate monomers with increased spacer length between amide and acrylate functionalities. This trend

follows the order of conformational flexibility of methylamide acrylate monomers as increasing spacer length between acrylate and amide functionalities entropically disfavours dimerization.³⁰ This was confirmed *via* self-association constant (K_a) determination using a literature model (Fig. 1C, eqn (S1)†) which proved MAmBA to possess the lowest K_a (0.38 M⁻¹). Moreover, all K_a values reported were within the expected range of other methylamide acrylates.³⁰

Polymer synthesis and characterisation

RAFT polymerisation was used to synthesise P(MAmA) homopolymers (Fig. 2A) in accordance to previous literature.³² A library of homopolymers were synthesised with varying degrees of polymerisation (DP_n) using BCTP as the chain transfer agent (CTA) and AsAc/tBuOOH as the redox pair. ¹H NMR and SEC characterisation of the purified products confirmed the successful synthesis of well-defined P(MAmAs) with low molar-mass dispersities ($D_M < 1.18$) and high monomer conversion obtained for all polymerisations (>95%) (Fig. 2B, C and Table 1). ¹³C NMR analysis confirmed successful polymerisations *via* introduction of signal C_a at 65 ppm (Fig. S6†).

Thermal properties in bulk

Previously, the thermal properties of P(MAmEA) were investigated by TGA and DSC, which revealed a stepwise decomposition and a T_g around room temperature, respectively.³² Here, TGA and DSC analyses were performed for P(MAmPA)₉₇ and P(MAmBA)₉₉.

TGA analysis illustrated two significant weight loss transitions of approximately 45 wt% for each of them (Fig. 3A). The first stepwise decomposition is observed with an onset temperature of 260 °C and 280 °C for P(MAmPA)₉₇ and P(MAmBA)₉₉ respectively, attributed to ester bond cleavage in the polymeric repeating unit. The second stepwise decomposition is observed with an onset temperature of 375 °C and 380 °C for P(MAmPA)₉₇ and P(MAmBA)₉₉ respectively, corresponding to the polymer backbone breakdown. For each weight loss transition, P(MAmBA)₉₉ showed the highest onset temperatures. Therefore, the thermal stability of P(MAmAs) can be enhanced by increasing the spacer length between functionalities. DSC analysis of P(MAmPA)₉₇ and P(MAmBA)₉₉ (Fig. 3B) revealed their amorphous character with T_g values being observed, which are high relative to other polyacrylates.^{34,35} Amongst them, P(MAmBA)₉₉ was found to have the lowest T_g value. An increase in chain mobility and simultaneous decrease in T_g was observed upon increasing spacer length between functionalities of P(MAmAs). This trend compliments the data in Fig. 1C as P(MAmBA)₉₉'s low T_g is due to a lower magnitude of intermolecular hydrogen-bonding, and higher side chain flexibility. Furthermore, this trend is significant as, in conjunction with TGA analysis, T_g and thermal properties of P(MAmAs) can be tuned as a function of the polymer side chain structure.

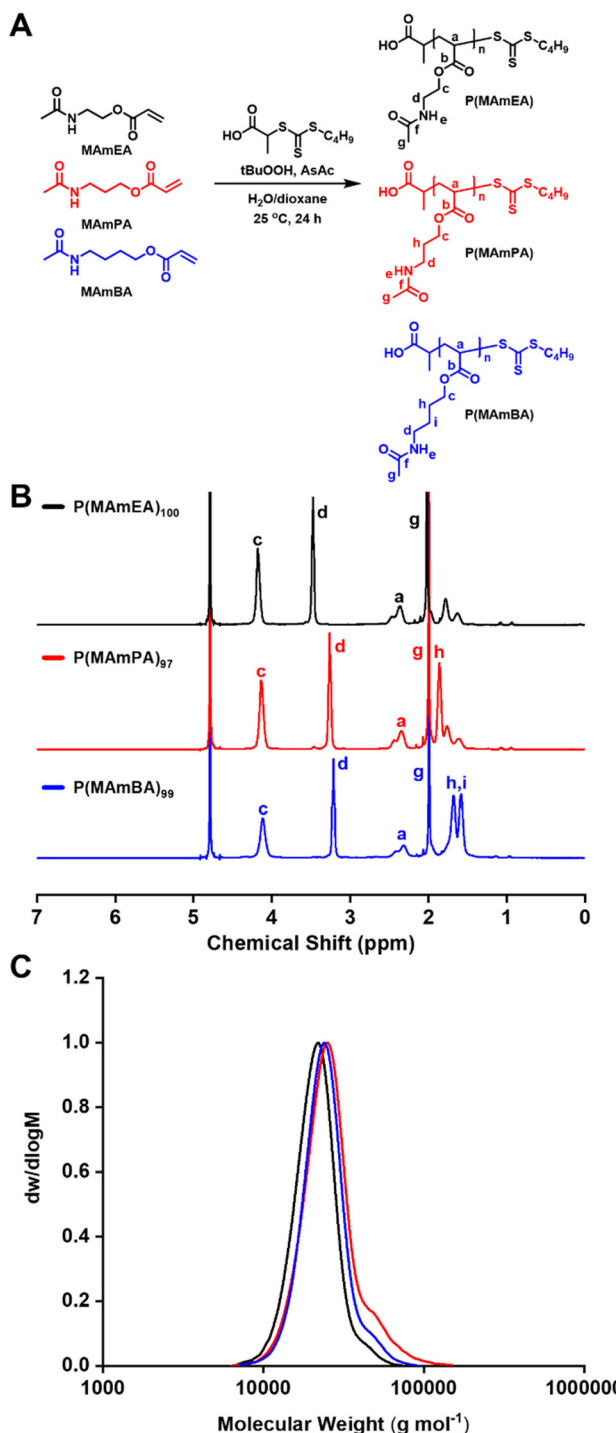


Fig. 2 (A) Synthesis pathway of homopolymers; (B) ¹H NMR spectra of P(MAmEA)₁₀₀, P(MAmPA)₉₇ and P(MAmBA)₉₉; (C) SEC traces of P(MAmEA)₁₀₀ ($M_n = 20\,000$, $D_M = 1.10$), P(MAmPA)₉₇ ($M_n = 23\,900$, $D_M = 1.17$) and P(MAmBA)₉₉ ($M_n = 22\,700$, $D_M = 1.12$).

Aqueous solubility: lower critical solution temperature (LCST) behaviour

Kempe *et al.*, previously reported the solubility of P(MAmEA)₁₀₀ in phosphate-buffered saline (PBS) (5.0 mg ml⁻¹, pH 7.4), which proved to be soluble over a temperature range

of 10–90 °C.³² However, they also found that the substitution of the methyl amide (P(MAmEA)₁₀₀) with ethyl amide groups (P(EAmEA)₁₀₀) while keeping the spacer length constant led to a LCST behaviour. Here, P(MAmEA)₁₀₀, P(MAmPA)₉₇ and P(MAmBA)₉₉ (5.0 mg ml⁻¹, PBS pH 7.4) were compared to investigate if increasing spacer length between amide and acrylate functionalities of P(MAmA) homopolymers had an effect on the thermoresponsive behaviour of these polymers. Whilst P(MAmEA)₁₀₀ and P(MAmPA)₉₇ were found to be soluble over a temperature range of 30–80 °C, P(MAmBA)₉₉ exhibited a LCST behaviour with a T_{cp} of 52.8 °C, confirming that thermo-responsive P(MAmAs) can be synthesised (Fig. 4, Table S2†). This data compliments the preceding monomer self-association data in Fig. 1C as the aqueous solubility of P(MAmAs) is heavily correlated to the alkyl spacer length between functionalities and the associated magnitude of intermolecular hydrogen-bonding. Furthermore, one can propose that if methylamide acrylate monomers possess K_a values greater than 0.52 M⁻¹ in CDCl₃, as shown in MAmEA and MAmPA, their resultant homopolymers (DP_n ~ 100) will exhibit excellent aqueous solubility. Conversely, if methylamide acrylate monomers possess K_a values lower than 0.38 M⁻¹ in CDCl₃, as present in MAmBA, their resultant homopolymers will exhibit reduced aqueous solubility at elevated temperatures thus giving rise to thermoresponsive polymers which display LCST behaviour.

This is likely due to the aforementioned increased conformational flexibility of MAmBA, which facilitates P(MAmBA) to undergo a coil-to-globule transition at elevated temperatures *via* an entropy increase. Moreover, a combination of increased intermolecular hydrophobic interactions between P(MAmBA) side chains, and simultaneous reduced solvation of P(MAmBA) side chains with water result in the polymer crashing out of solution.³⁶ These results demonstrate that increasing the spacer length has a less pronounced effect on the aqueous solubility compared to changing the peripheral amide group of the side chain, as P(EAmEA)₁₀₀ shows a T_{cp} of 26.6 °C in identical conditions.³²

To further investigate the thermoresponsive and LCST behaviour of P(MAmBA), a series of turbidity experiments was performed on P(MAmBA) solutions to investigate the effect of DP_n, concentration and media on observed T_{cp} 's. Previous literature has found that lowering the DP_n of thermo-responsive polymers directly corresponds to a decrease in their observed T_{cp} .³⁷ Furthermore, altering both concentration³⁷ and media³⁸ of the polymer solutions has been found to have similar effects. Notably, these observations are consistent with PNIPAm which similar to P(MAmBA) possesses a side-chain pendant amide functionality.^{39–42}

To investigate the effect of DP_n on T_{cp} , P(MAmBA) was synthesised at four different DP_n (DP_n = 25, 48, 99, 190). ¹H NMR and SEC analysis confirmed successful synthesis of these homopolymers (Table 1, Fig. S7†). Each homopolymer was subsequently dissolved in PBS to produce 5 mg ml⁻¹ solutions, which were analysed *via* turbidity measurements over a temperature range of 30–80 °C. Of the four solutions; P(MAmBA)₁₉₀, P(MAmBA)₉₉ and P(MAmBA)₄₈ displayed T_{cp} values of 39.6 °C,

Table 1 Characterisation of the synthesised homopolymers

Sample	Target DP _n	Conversion (%)	Actual DP _n ^a	M _{n, th} ^b (g mol ⁻¹)	M _{n, SEC} ^c (g mol ⁻¹)	D _M ^c	T _g ^d (°C)	T _{cp} ^e (°C)
P(MAmEA) ₁₀₀	100	100	100	16 000	20 000	1.10	N.d.	—
P(MAmPA) ₉₇	100	97	97	16 800	23 900	1.17	20.1	—
P(MAmBA) ₂₅	25	100	25	4900	8200	1.12	8.9	—
P(MAmBA) ₄₈	50	96	48	9100	13 800	1.12	11.1	66.0
P(MAmBA) ₉₉	100	99	99	18 600	22 700	1.11	14.0	52.8
P(MAmBA) ₁₉₀	200	95	190	35 400	46 300	1.12	N.d.	39.6

^a Calculated by ¹H NMR (D₂O, 400 MHz) from target DP_n and conversion. ^b Calculated from DP_n and molar masses of monomers and CTA.

^c Determined by SEC (eluent: DMF, calibration standard: PMMA). ^d Determined by DSC (second heating run). ^e Cloud point temperature (5 mg ml⁻¹, PBS) in the temperature range 30–80 °C. n.d. = not determined.

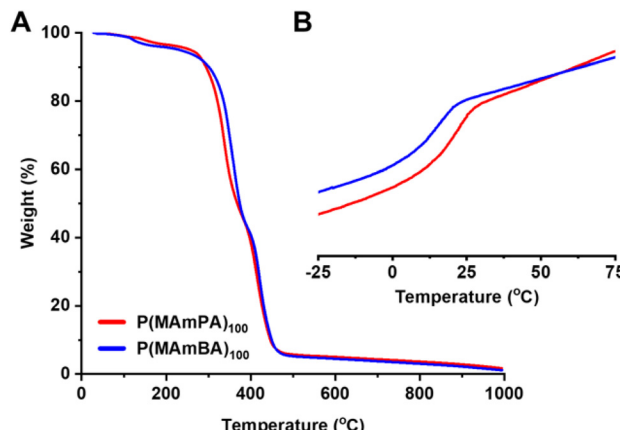


Fig. 3 (A) TGA traces of P(MAmPA)₉₇ and P(MAmBA)₉₉; (B) DSC measurements of P(MAmPA)₉₇ ($T_g = 20.1$ °C) and P(MAmBA)₉₉ ($T_g = 14.0$ °C).

52.8 °C and 66.0 °C respectively whilst P(MAmBA)₂₅ was soluble over the temperature range investigated (Fig. 4A, Table 1). This data not only suggests homopolymer T_{cp} can be lowered by increasing side chain length, concordant with previous literature,^{37,39} but that there is a critical chain length required for LCST behaviour to be observed for P(MAmBA); 25 < DP_n < 48. Furthermore, increasing P(MAmBA) M_n was shown to have a greater effect on observed T_{cp} values than PNIPAm. This was evident by comparing the preceding data to studies by Stöver *et al.*, which showed increasing PNIPAm M_n from 2800 g mol⁻¹ to 26 500 g mol⁻¹ only reduced observed T_{cp} values by ~10.0 °C.³⁹

To investigate the effect of concentration on T_{cp} , solutions of P(MAmBA)₉₉ were prepared in PBS at three concentrations; 5 mg ml⁻¹, 1 mg ml⁻¹ and 0.1 mg ml⁻¹. Lowering the concentration from 5 mg ml⁻¹ to 1 mg ml⁻¹ resulted in a slight increase of T_{cp} 's from 52.8 °C to 57.2 °C (Fig. 4A, Table S2†). Furthermore, the steepness of the sigmoidal trace observed lowered upon dilution, indicating the phase transition of P(MAmBA)₉₉ occurs over a wider temperature range at lower concentrations. Upon further diluting the P(MAmBA)₉₉ solution to a concentration of 0.1 mg ml⁻¹, macroscopic precipitation was not observed over the measured temperature range, indicating LCST behaviour is either not observed at this con-

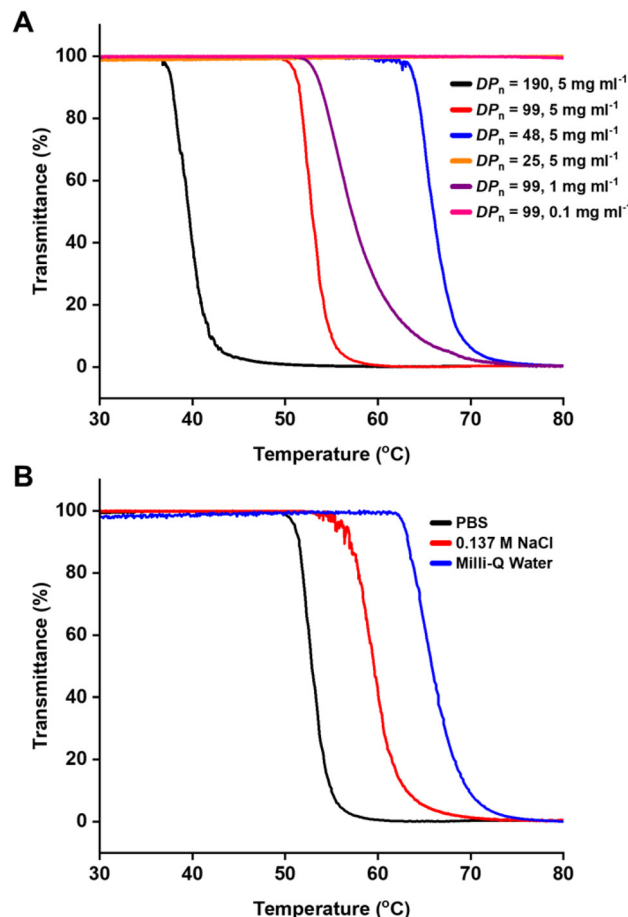


Fig. 4 Turbidity measurements of (A) PBS solutions of P(MAmBA) of different DP_n and concentrations; and (B) P(MAmBA)₉₉ solutions in different media (5 mg ml⁻¹).

centration or occurs at temperatures >80 °C (Fig. 4A, Table S2†). Therefore, increasing the concentration of P(MAmBA) in solution directly lowers its observed T_{cp} , which is consistent with previous literature on thermoresponsive polymers.³⁷ Moreover, the effect of concentration on P(MAmBA)₉₉ aqueous solubility is much more pronounced than on PNIPAm, where increasing concentration from 1 mg ml⁻¹ to 50 mg ml⁻¹ was only found to reduce observed T_{cp} values by ~2.0 °C.⁴⁰

Subsequent turbidity measurements were performed on solutions of P(MAmBA)_{99} (5 mg ml⁻¹) in three different media to investigate the effect of salts present in aqueous solutions on T_{cp} ; Milli-Q water, PBS and 0.137 M sodium chloride (NaCl) (Fig. 4B, Table S2†). A 0.137 M NaCl solution was prepared due to its equal molarity to that of the PBS solution used to investigate the sole effect of NaCl on P(MAmBA) solubility. T_{cp} values of 65.8 °C, 59.6 °C and 52.8 °C were observed for Milli-Q water, 0.137 M NaCl and PBS solutions respectively (Fig. 4B, Table S2†). The Milli-Q water solution displayed the highest T_{cp} of the three solutions (65.9 °C), indicating the presence of salts in aqueous solutions of P(MAmBA)_{99} has a pronounced effect on its solubility. This is consistent with previous research on the influence of salts on polymer-water interactions, as summarised by the Hofmeister series.^{41,43–45} Salt effects the hydrogen-bonds between polymer chains and water molecules thus LCST behaviour can be affected. This was exemplified as the T_{cp} value of the 0.137 M NaCl solution (59.6 °C) was lower compared to the Milli-Q water solution (65.8 °C), indicating an aqueous solution of 0.137 M NaCl provides sufficient salt to disrupt hydrogen-bonds between polar groups of P(MAmBA)_{99} side chains and water molecules at elevated temperatures.⁴⁶ This observation is consistent with previous literature on other thermoresponsive poly(acrylate)s, which stated increasing the concentration of NaCl in aqueous solutions directly reduces their measured LCST values.²⁶ Moreover, the differences in T_{cp} values between the 0.137 M NaCl solution (59.6 °C) and the PBS solution (52.8 °C) can be attributed to the magnitude of the salting-out effect present. This is because the PBS solution used is comprised of four salts; 0.002 M dipotassium phosphate, 0.008 M disodium phosphate, 0.0027 M potassium chloride and 0.137 M NaCl. Therefore, the increased salt content in PBS further disrupts P(MAmBA)_{99} -water interactions relative to 0.137 M NaCl, resulting in a lower T_{cp} . Moreover, increasing salt content was found to have larger effect on P(MAmBA) 's observed T_{cp} value than PNIPAm. This is because 0.2 M Hofmeister ion solutions of PNIPAm have proved to only reduce T_{cp} values by <5.0 °C relative to their salt-free solutions, irrespective to M_n .^{41,42}

Overall, the series of turbidity measurements performed proved that one can utilise a number of variables (DP_n , concentration and media) to tune the T_{cp} of thermoresponsive P(MAmA) s to a desired application. Moreover, the magnitude of hydrogen-bonding (K_a) of methylamide acrylate monomers directly influences the aqueous solubility of their corresponding homopolymers.

Surface property analysis

To further investigate the hydrophilicity of the synthesised P(MAmA) s ($DP_n \sim 100$), surface property analysis was performed *via* water contact angle (CA) measurements. Polymeric films of each homopolymer were prepared on glass slides using a spin-coating methodology to prepare uniform films. P(MAmEA)_{100} , P(MAmPA)_{97} and P(MAmBA)_{100} displayed water contact angles at ambient temperature (25 °C) of $11.0 \pm 0.2^\circ$, $11.6 \pm 0.3^\circ$ and $12.0 \pm 0.5^\circ$ respectively (Fig. 5A), confirming

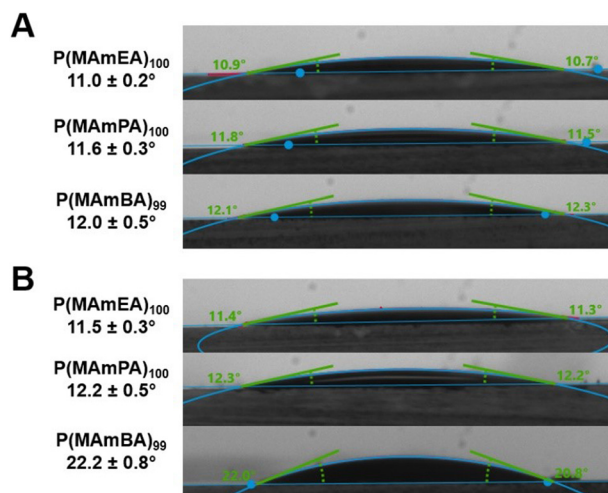


Fig. 5 (A) Water contact angle images of P(MAmEA)_{100} , P(MAmPA)_{97} and P(MAmBA)_{99} at 25 °C; (B) water contact angle images of P(MAmEA)_{100} , P(MAmPA)_{97} and P(MAmBA)_{99} at 75 °C.

their hydrophilic nature compared to a control (uncoated glass slide, $59.0 \pm 2.7^\circ$, Fig. S8†).

Whilst all polymeric films exhibited similar contact angles at ambient temperature, this procedure was repeated at an elevated temperature (75 °C) to further investigate the thermo-responsive behaviour of P(MAmA) s. At 75 °C, P(MAmEA)_{100} , P(MAmPA)_{97} and P(MAmBA)_{100} displayed water contact angles of $11.5 \pm 0.3^\circ$, $12.2 \pm 0.5^\circ$ and $22.2 \pm 0.8^\circ$ respectively (Fig. 5B). Therefore, only P(MAmBA) exhibited a significant increase (+10.2°) in observed contact angles at elevated temperatures, further confirming its thermo-responsive nature compared to P(MAmEA) and P(MAmPA) . Moreover, this data indicates increasing spacer length between the polymer backbone and amide functionality decreases the magnitude of hydrophilicity observed for P(MAmA) s, concordant with our aqueous solubility measurements.

Conclusions

In summary, we report the successful synthesis of three methylamide acrylate monomers with varying spacer lengths between functionalities, and their subsequent RAFT polymerisations to yield well-defined P(MAmA) homopolymers (conversion > 95%, $D_m < 1.17$). The magnitude of intermolecular hydrogen-bonding in these monomers was assessed whereby the monomer with the largest spacer length between functionalities, MAmBA, was found to possess the lowest K_a (0.37 M⁻¹). Thermal analysis proved all homopolymers to be amorphous in nature with high glass-transition temperatures observed ($T_g > 14.0$ °C) relative to other polyacrylates.^{34,35} Furthermore, P(MAmBA)_{99} possessed the lowest T_g attributed to higher flexibility and lower hydrogen-bonding between polymer side chains. Each homopolymer was found to thermally degrade *via* a two-step decomposition whereby increas-

ing spacer length corresponded to an increase in observed onset decomposition temperatures. Aqueous solubility analysis of the synthesised homopolymers revealed P(MAmBA) to be the only homopolymer which exhibited LCST behaviour, complimenting preceding monomer self-association data. Further investigation into P(MAmBA)'s solubility behaviour found an increase in concentration and DP_n directly correlates to a decrease in observed T_{cp} values. Moreover, the presence of salts in aqueous solutions was found to have a pronounced effect on P(MAmBA) solubility. These findings prove the spacer length between functionalities in methylamide monomers has significant influence on the thermal properties and aqueous solubility of their corresponding homopolymers with the potential to induce LCST behaviour. This is highly interesting in the context of synthesising novel water-soluble thermo-responsive polymers for biomedical applications. Furthermore, the high thermal stability of P(MAmBA) coupled with its facile T_{cp} tunability relative to PNIPAM make the homopolymer a promising candidate which justifies further exploration.

Author contributions

The manuscript was written through contributions of all authors. All authors have approved the submitted version of the manuscript.

Conflicts of interest

There are no conflicts to declare.

Acknowledgements

The authors acknowledge the technical assistance of the University of Warwick Polymer Characterisation RTP team. P. W. thanks the Royal Society and Tata companies for the award of a University Research Fellowship (URF\R1\180274). K.K. gratefully acknowledges the award of an ARC Future Fellowship (FT190100572) from the Australian Research Council (ARC). A.R. wishes to acknowledge the Monash Graduate Scholarship and Monash International Tuition Scholarship.

References

- 1 B. L. Rivas, E. Pereira and A. Maureira, *Polym. Int.*, 2009, **58**, 1093–1114.
- 2 K. Halake, M. Birajdar, B. S. Kim, H. Bae, C. C. Lee, Y. J. Kim, S. Kim, H. J. Kim, S. Ahn, S. Y. An and J. Lee, *J. Ind. Eng. Chem.*, 2014, **20**, 3913–3918.
- 3 B. L. Rivas, E. D. Pereira, M. Palencia and J. Sánchez, *Prog. Polym. Sci.*, 2011, **36**, 294–322.
- 4 V. G. Kadajji and G. V. Betageri, *Polymers.*, 2011, **3**, 1972–2009.
- 5 T. Berninger, N. Dietz and Ó. González López, *Microb. Biotechnol.*, 2021, **14**, 1881–1896.
- 6 S. Perrier, *Macromolecules*, 2017, **50**, 7433–7447.
- 7 K. Matyjaszewski, *Macromolecules*, 2012, **45**, 4015–4039.
- 8 A. Anastasaki, V. Nikolaou, G. Nurumbetov, P. Wilson, K. Kempe, J. F. Quinn, T. P. Davis, M. R. Whittaker and D. M. Haddleton, *Chem. Rev.*, 2016, **116**, 835–877.
- 9 J. Nicolas, Y. Guillaneuf, C. Lefay, D. Bertin, D. Gigmes and B. Charleux, *Prog. Polym. Sci.*, 2013, **38**, 63–235.
- 10 F. Doberenz, K. Zeng, C. Willems, K. Zhang and T. Groth, *J. Mater. Chem. B*, 2020, **8**, 607–628.
- 11 A. Bordat, T. Boissenot, J. Nicolas and N. Tsapis, *Adv. Drug Delivery Rev.*, 2019, **138**, 167–192.
- 12 Y. J. Kim and Y. T. Matsunaga, *J. Mater. Chem. B*, 2017, **5**, 4307–4321.
- 13 N. Deirram, C. Zhang, S. S. Kermanian, A. P. R. Johnston and G. K. Such, *Macromol. Rapid Commun.*, 2019, **40**, 1–23.
- 14 G. Kocak, C. Tuncer and V. Bütün, *Polym. Chem.*, 2017, **8**, 144–176.
- 15 O. Bertrand and J. F. Gohy, *Polym. Chem.*, 2017, **8**, 52–73.
- 16 T. Manouras and M. Vamvakaki, *Polym. Chem.*, 2017, **8**, 74–96.
- 17 Q. Zhang, C. Weber, U. S. Schubert and R. Hoogenboom, *Mater. Horiz.*, 2017, **4**, 109–116.
- 18 J. Seuring and S. Agarwal, *ACS Macro Lett.*, 2013, **2**, 597–600.
- 19 A. Halperin, M. Kröger and F. M. Winnik, *Angew. Chem., Int. Ed.*, 2015, **54**, 15342–15367.
- 20 L. Tang, L. Wang, X. Yang, Y. Feng, Y. Li and W. Feng, *Prog. Mater. Sci.*, 2021, **115**, 100702.
- 21 H. Cheng, L. Shen and C. Wu, *Macromolecules*, 2006, **39**, 2325–2329.
- 22 K. Uchida, K. Sakai, E. Ito, O. H. Kwon, A. Kikuchi, M. Yamato and T. Okano, *Biomaterials*, 2000, **21**, 923–929.
- 23 Y. Zhang, J. Cai, C. Li, J. Wei, Z. Liu and W. Xue, *J. Mater. Chem. B*, 2016, **4**, 3733–3749.
- 24 Q. Li, A. P. Constantinou and T. K. Georgiou, *J. Polym. Sci.*, 2021, **59**, 230–239.
- 25 N. Badi, *Prog. Polym. Sci.*, 2017, **66**, 54–79.
- 26 S. N. Nishimura, K. Nishida, T. Ueda, S. Shiromoto and M. Tanaka, *Polym. Chem.*, 2022, **13**, 2519–2530.
- 27 N. Yan, J. Zhang, Y. Yuan, G. T. Chen, P. J. Dyson, Z. C. Li and Y. Kou, *Chem. Commun.*, 2010, **46**, 1631–1633.
- 28 R. Hoogenboom and H. Schlaad, *Polym. Chem.*, 2017, **8**, 24–40.
- 29 F. Biryani and K. Demirelli, *Ferroelectrics*, 2018, **526**, 76–94.
- 30 L. Voorhaar, E. W. C. Chan, P. Baek, M. Wang, A. Nelson, D. Barker and J. Travas-Sejdic, *Eur. Polym. J.*, 2018, **105**, 331–338.
- 31 Y. Chen and Z. Guan, *Chem. Commun.*, 2014, **50**, 10868–10870.

32 A. M. Mahmoud, J. P. Morrow, D. Pizzi, S. Nanayakkara, T. P. Davis, K. Saito and K. Kempe, *Macromolecules*, 2020, **53**, 693–701.

33 M. P. Williamson, *Prog. Nucl. Magn. Reson. Spectrosc.*, 2013, **73**, 1–16.

34 F. Fleischhaker, A. P. Haehnel, A. M. Misske, M. Blanchot, S. Haremza and C. Barner-Kowollik, *Macromol. Chem. Phys.*, 2014, **215**, 1192–1200.

35 W. Liu and C. Cao, *Colloid Polym. Sci.*, 2009, **287**, 811–818.

36 G. Pasparakis and C. Tsitsilianis, *Polymer*, 2020, **211**, 123146.

37 R. Hoogenboom, H. M. L. Thijs, M. J. H. C. Jochems, B. M. Van Lankveld, M. W. M. Fijten and U. S. Schubert, *Chem. Commun.*, 2008, 5758–5760.

38 N. ten Brummelhuis, C. Secker and H. Schlaad, *Macromol. Rapid Commun.*, 2012, **33**, 1690–1694.

39 Y. Xia, X. Yin, N. A. D. Burke and H. D. H. Stöver, *Macromolecules*, 2005, **38**, 5937–5943.

40 S. Furyk, Y. Zhang, D. Ortiz-Acosta, P. S. Cremer and D. E. Bergbreiter, *J. Polym. Sci., Part A: Polym. Chem.*, 2006, **44**, 1492–1501.

41 Y. Zhang, S. Furyk, L. B. Sagle, Y. Cho, D. E. Bergbreiter and P. S. Cremer, *J. Phys. Chem. C*, 2007, **111**, 8916–8924.

42 Y. Zhang, S. Furyk, D. E. Bergbreiter and P. S. Cremer, *J. Am. Chem. Soc.*, 2005, **127**, 14505–14510.

43 E. Thormann, *RSC Adv.*, 2012, **2**, 8297–8305.

44 B. Kang, H. Tang, Z. Zhao and S. Song, *ACS Omega*, 2020, **5**, 6229–6239.

45 S. Z. Moghaddam and E. Thormann, *J. Colloid Interface Sci.*, 2019, **555**, 615–635.

46 K. Van Durme, H. Rahier and B. Van Mele, *Macromolecules*, 2005, **38**, 10155–10163.